Burns & Trauma, 2026, **14**, tkaf073
https://doi.org/10.1093/burnst/tkaf073
Advance access publication date 6 November 2025
Research Article

H3K56 lactylation promotes collagen II synthesis to modulate chondrocyte metabolism in posttraumatic osteoarthritis

Zicai Dong[1,‡], Di Liu[2,‡], Guangyun Hu[3], Zeyu Yang[4], Qin Shu[3], Qijie Dai[5], Hao Tang[1], Chuan Yang[1], Chunrong Zhao[1], Xiaoshan Gong[1], Rujie Wang[6], Weikai Kong[7], Shiwu Dong[1,8,*]

[1]Department of Biomedical Materials Science, Third Military Medical University (Army Medical University), Gaotanyan Street no. 30, Shapingba District, Chongqing 400038, China
[2]Department of Trauma Medical Center, State Key Laboratory of Trauma and Chemical Poisoning, Daping Hospital, Third Military Medical University (Army Medical University), Changjiang Road no. 10, Yuzhong District, Chongqing 400042, China
[3]Department of Field Nursing, School of Nursing, Third Military Medical University (Army Medical University), Gaotanyan Street no. 30, Shapingba District, Chongqing 400038, China
[4]Department of Breast and Thyroid Surgical Department, Chongqing General Hospital, Xingguang Avenue no. 118, Liangjiang District, Chongqing 400013, China
[5]Department of Orthopedics, Southwest Hospital, Third Military Medical University (Army Medical University), Gaotanyan Street no. 30, Shapingba District, Chongqing 400038, China
[6]Department of Orthopedics, Xinqiao Hospital, Third Military Medical University (Army Medical University), Xinqiao Street no. 83, Shapingba District, Chongqing 400030, China
[7]Department of Pathology, Southwest Hospital, Third Military Medical University (Army Medical University), Gaotanyan Street no. 30, Shapingba District, Chongqing 400038, China
[8]State Key Laboratory of Trauma and Chemical Poisoning, Third Military Medical University (Army Medical University), Changjiang Road no. 10, Yuzhong District, Chongqing 400038, China

*Corresponding author. E-mail: dongshiwu@tmmu.edu.cn

‡These authors contributed equally to this work.

Abstract

Background: The accumulation of intracellular glycolytic lactate is a hallmark characteristic of chondrocytes. Histone lactylation, a post-translational modification mediated by lactate, plays a pivotal role in regulating the physiological functions of chondrocytes and contributes to the pathogenesis of posttraumatic osteoarthritis. This study was designed to investigate the role of glycolytic lactate-dependent histone H3 lysine 56 lactylation (H3K56la) in modulating the synthesis of type II collagen in chondrocytes. Furthermore, through a combination of laboratory-based and animal experimental approaches, the study sought to uncover new insights into potential therapeutic strategies for the management of posttraumatic osteoarthritis.
Methods: In in vitro experiments, the researchers first conducted assays to inhibit and induce histone lactylation in chondrocytes, subsequently measuring changes in the expression levels of hypoxia-inducible factor 1 alpha (HIF 1α) and the type II collagen alpha 1 chain gene (Col2a1). Next, we assessed alterations in intracellular lactylation levels and Col2a1 expression following either knockdown or overexpression of HIF 1α in chondrocytes. To further elucidate the regulatory relationship between HIF 1α and Col2a1, chromatin immunoprecipitation assays were performed to investigate the transcriptional control exerted by HIF 1α on the Col2a1 gene promoter. In addition, murine models of posttraumatic osteoarthritis were developed using anterior cruciate ligament transection surgery. Both *in vivo* and *in vitro* experiments were then carried out to explore the chondroprotective mechanisms and therapeutic potential associated with modulation of histone lactylation in chondrocytes.
Results: Induction of histone lactylation in chondrocytes led to a significant upregulation of HIF 1α expression. Conversely, knockdown of HIF 1α resulted in a marked reduction in both H3K56 lactylation and Col2a1 expression. It was found that H3K56la and HIF 1α functioned synergistically to positively regulate collagen synthesis, with HIF 1α directly binding to the promoter region of the Col2a1 gene to enhance its transcription. Treatment with α-ketoglutarate modified the cellular redox state and contributed to increased expression of both H3K56la and Col2a1.
Conclusions: The glycolytic lactate/H3K56la/HIF 1α regulatory axis plays a positive regulatory role in the synthesis of type II collagen in chondrocytes by facilitating the binding of HIF 1α to the Col2a1 gene promoter. Activation of this molecular pathway holds promise as a novel therapeutic strategy for the treatment of posttraumatic osteoarthritis.

Keywords: Chondrocyte; Collagen II; Histone lactylation; H3K56la; HIF 1α; Posttraumatic osteoarthritis

Highlights

1. This study reveals lactate-dependent histone H3K56 lactylation as a key upstream regulator activating HIF 1α to drive Col2a1 synthesis in chondrocytes.
2. HIF 1α binds the *Col2a1* gene promoter, forming a positive regulating axis where increased H3K56la/HIF 1α expression directly enhances collagen production.
3. Modulating chondrocyte redox state with α-ketoglutarate boosts H3K56la and Col2a1 expression, suggesting a novel metabolic approach for post-traumatic osteoarthritis therapy.

Received: July 17, 2025. **Revised:** November 2, 2025. **Accepted:** November 5, 2025
© The Author(s) 2025. Published by Oxford University Press.
This is an Open Access article distributed under the terms of the Creative Commons Attribution-NonCommercial License (https://creativecommons.org/licenses/by-nc/4.0/), which permits non-commercial re-use, distribution, and reproduction in any medium, provided the original work is properly cited. For commercial re-use, please contact reprints@oup.com for reprints and translation rights for reprints. All other permissions can be obtained through our RightsLink service via the Permissions link on the article page on our site—for further information please contact journals.permissions@oup.com.

Downloaded from academic.oup.com/burnstrauma/article/doi/10.1093/burnst/tkaf073/8315826 by guest on 12 October 2026

Background

Posttraumatic osteoarthritis (PTOA) represents a significant global health challenge, with ~5.6 million new cases diagnosed each year and a prevalence rate of 21.1% among individuals who have previously sustained joint injuries. Recent epidemiological studies indicate a concerning upward trend in PTOA incidence between 2000 and 2022, with forecasts suggesting that its prevalence could nearly double to 40.6% by the year 2030 [1]. Distinct from primary osteoarthritis, which typically arises due to age-related wear and tear, PTOA primarily affects younger populations following high-energy traumatic events such as motor vehicle collisions, military combat injuries, and sports-related mishaps [2]. These traumatic incidents initiate a cascade of complex pathophysiological processes that go well beyond the initial mechanical damage [3]. The pathogenesis of PTOA is characterized by immediate structural joint damage followed by progressive cartilage deterioration. This progression underscores the importance of early therapeutic intervention, particularly within the acute phase of trauma care. Understanding the early molecular and cellular events following injury is essential for developing effective preventive and therapeutic strategies.

Current research has shown that chondrocytes adapt to the avascular cartilage environment by relying predominantly on glycolytic metabolism, generating lactate as both an energy substrate and a signalling molecule [4]. Synovial fluid lactate has been identified as a diagnostic biomarker, with elevated concentrations observed in the contexts of septic arthritis and inflammatory joint conditions. Recent investigations have revealed that lactate functions as both a metabolic substrate and signalling molecule through hydroxy-carboxylic acid receptor 1 (HCAR1), which activates the PI3K/Akt pathway, leading to the upregulation of NADPH oxidase 4 (NOX4) expression and the generation of reactive oxygen species [5]. Histone lactylation is a novel epigenetic mechanism that regulates gene transcription in chondrocytes. Studies have demonstrated that lactate dehydrogenase A (LDHA)-mediated H3K18 lactylation influences osteoarthritis progression through the transcriptional regulation of glycolytic enzymes, including TPI1 [6]. Several studies have demonstrated the importance of specific lactylation sites, with H3K18 lactylation found to promote chondrogenic differentiation and cartilage matrix deposition in organoid models [7], whereas H3K18 lactylation has been implicated in osteoarthritis progression through LDHA-mediated mechanisms [6]. The transcription factor hypoxia-inducible factor 1 alpha (HIF 1α) has been identified as a central regulator of chondrocyte adaptation to hypoxic conditions, controlling both metabolic reprogramming and extracellular matrix synthesis [8]. However, the precise molecular mechanisms governing lactate-mediated H3K56 lactylation and its interaction with HIF 1α in the setting of traumatic cartilage injury remain incompletely characterized.

Despite the considerable progress in understanding chondrocyte metabolism and epigenetic regulation, critical knowledge gaps remain regarding the therapeutic modulation of lactate-dependent histone modifications in posttraumatic cartilage degeneration [9]. Current osteoarthritis treatments leave patients largely symptomatic, and they exhibit a limited capacity to halt or reverse disease progression [10]. This therapeutic limitation is particularly concerning for the treatment of PTOA, where early intervention opportunities exist within defined therapeutic windows following joint injury [11, 12]. α-Ketoglutarate (αKG) has been shown to protect against osteoarthritis through multiple mechanisms, including mitophagy regulation, oxidative stress reduction, and anti-inflammatory activities via IKK/NF-κB pathway inhibition [13, 14]. Recent clinical investigations have established the efficacy of αKG in preserving cartilage integrity and reducing joint inflammation in both natural ageing and surgically induced osteoarthritis models [15, 16]. However, the molecular mechanisms underlying its therapeutic efficacy remain incompletely characterized, particularly regarding its interaction with cellular redox status and lactate-mediated epigenetic modifications. Furthermore, the complex interplay among cellular redox status, lactate shuttling, and histone lactylation presents both opportunities and challenges for therapeutic intervention in PTOA.

In this study, we explored the role of lactate-mediated histone modifications in the mechanisms underlying traumatic cartilage injury and subsequent repair processes. We found that trauma-induced oxidative stress disrupts normal chondrocyte metabolism, leading to altered lactate levels and subsequent changes in histone lactylation. Our findings demonstrate the existence of a glycolytic lactate/H3K56la/HIF 1α positive-regulatory axis that promotes type II collagen synthesis in chondrocytes through transcriptional regulation. Furthermore, we established that αKG treatment modulates cellular redox status by increasing NADH and NADPH production, promotes the influx of extracellular lactate, and activates this protective pathway through direct binding of HIF 1α to the Col2a1 gene promoter while protecting chondrocytes from oxidative stress-induced apoptosis. These insights uncover a mechanistic link between redox metabolism and epigenetic regulation via lactate-mediated histone modifications, providing a deeper understanding of how αKG exerts its therapeutic effects. Importantly, our findings highlight the potential for targeting the glycolytic lactate/H3K56la/HIF 1α axis as a novel therapeutic strategy for intervening in the early pathophysiological phases of posttraumatic joint degeneration, with the aim of preventing the onset or progression of PTOA.

Methods

Animal osteoarthritis model

8-week-old female C57BL/6 J mice were purchased from the Laboratory Animal Center of Army Medical University (production license number: SCXK (yu)2022–0011). After 2 days of acclimation, the mice were randomly divided into four groups. Three experimental groups (n = 5 each) underwent anterior cruciate ligament transection (ACLT) operations under 5% pentobarbital sodium anesthesia to induce osteoarthritis models for further study. The sham-operated group (n = 5) served as a control and underwent the same procedure except ACLT. All animals in the respective groups were housed in individually ventilated cages (IVCs) in a cozy environment with a temperature of 25 ± 2°C and humidity of 50 ± 10%. They had free access to food and water, and a 12-hour light/dark cycle. All experimental procedures were approved by the Committee on the Use and Care of Animals at Army Medical University and were conducted according to the Guidelines for the Care and Use of Experimental Animals of the National Institute of Health (animal ethical statement number: AMUWEC20226055).

Downloaded from academic.oup.com/burnstrauma/article/doi/10.1093/burnst/tkaf073/8315826 by guest on 12 October 2026

Isolation and culture of mouse chondrocytes and cardiomyocytes

Primary chondrocytes were isolated from the healthy distal femur and tibial plateau articular cartilage of 5-day-old female C57BL/6 J mice, and primary cardiomyocytes were isolated from the heart. In brief, mice were sacrificed after anesthesia. The articular cartilage of the distal femur and tibial plateau, as well as the heart, were separated and cut into small pieces ~1 mm^3, then rinsed with PBS 3 times, digested with 0.25% trypsin for 60 min, plated in culture dishes containing 0.25% collagenase-IV at 37°C with 5% CO_2 for 6 h, and then filtrated through a 70 μm cell strainer. Cell suspensions were centrifuged at 1000 rpm for 5 min, resuspended in DMEM culture medium with 10% fetal bovine serum (FBS), and cultured at 37°C with 5% CO_2. An oxygen-controlled cell culture system was modified from T25 cell culture flasks with an airtight connection after seeding 2×10^6 chondrocytes. Cells were harvested after 24 hours of culture for subsequent experiments.

Cell proliferation assay

The cell viability of primary articular chondrocytes treated with various concentrations of specific inhibitors of glycolysis and enzymes, and αKG or TBHP was assessed with a cell counting kit-8 (CCK8) assay kit. Cells were seeded into 96-well plates and exposed to different concentrations of αKG (0–10 mM) or TBHP (0–200 μM) for 24, 48, or 72 hours. Then the cells were washed with 1 × PBS and incubated with serum-free medium containing 10% CCK8 reagent for 1 hour at 37°C with 5% CO_2. The absorbance at 450 nm was measured using a Bio-Tek, Synergy H4 microplate reader. All samples were analyzed in triplicate. The cell viability was calculated as $\left[(As - Ab) / (Ac - Ab)\right] \times 100\%$, where Ab is the absorbance of the blank group (medium only, without cells, αKG or TBHP), Ac is the absorbance of the control group (without αKG or TBHP), and As is the absorbance of the sample group (with various concentrations of αKG or TBHP).

Flow cytometry analysis

Flow cytometry was used to analyze the apoptosis rate of chondrocytes according to the Annexin V-FITC/PI apoptosis kit protocol (CA1020, Solarbio, China). Briefly, chondrocytes were incubated with or without 20 μM TBHP for 6 hours, and then treated with different concentrations of αKG for 48 hours. The cells were washed with PBS twice, digested with 0.25% EDTA -free trypsin (C0205, Beyotime, China), centrifuged at 1000 rpm for 3 min, and suspended in 1× binding buffer at a concentration of 1×10^6/ml. 100 μl suspension was stained with 5 μl of annexin V-FITC and 10 μl of 20 μg/ml PI. Cell apoptosis was measured using a CytoFLEX flow cytometer (Beckman Coulter, USA) and the data were analyzed with CytExpert and Kaluza software.

Histology and immunochemistry

Mouse knee specimens were decalcified with EDTA for 10 days after micro-CT scanning and washed with PBS to remove residual paraformaldehyde. After dehydration and paraffin embedding, 5 μm thick serial sections were made with a microtome (Leica RM2125 RTS) and stained for haematoxylin–eosin (HE), safranin O-fast green, and toluidine blue. Immunohistochemical staining was also performed to evaluate the relative intensity of Col2a1, Aggrecan, MMP13, and ADAMTS5. The stained sections were scanned with a slide-viewer (Olympus VS200), and the images were exported to quantify articular cartilage damage, thickness, and other indicators.

Immunofluorescence

After dewaxing the tissue sections, antigenic epitope retrieval was conducted in a microwave oven in EDTA-sodium citrate solution. The sections were blocked with 5% BSA at room temperature for 1 hour and then incubated with diluted primary antibody overnight at 4°C. A fluorescent secondary antibody of the species corresponding to the primary antibody was added and incubated for 2 hours protected from light. The same procedure was repeated with the second primary antibody and the corresponding secondary antibody. DAPI staining solution was then introduced and incubated for 30 min before the sections were analyzed by scanning in the VS200 slide-viewer. Sections were washed 3 times with PBS solution for 5 min before the next step.

Western blot analysis

Chondrocytes cytosolic protein and nuclear protein were extracted with RIPA buffer (P0013B, Beyotime, China) and nucleoprotein extraction reagent (R0050, Solarbio, China) containing protease and phosphatase inhibitors. For western blotting analysis, antibodies against Col2a1 (AF6528, Beyotime, China), ADAMTS5 (bs-3573R, Bioss, China), Aggrecan (AF6126, Beyotime, China), MMP13 (AF7479, Beyotime, China), β-actin (AF0003, Beyotime, China), Histone H3 (AF0009, Beyotime, China), Histone H4 (AF2581, Beyotime, China), Pan Kla (PTM-1401, PTM, China), Pan Kac (PTM-101, PTM, China), H3K56la (PTM-1421RM, PTM, China), HIF 1α (#36169, CST, USA), HIF 1α (AF7087,Beyotime, China), HIF 1α (Huabio, China) were used.

Enzyme-linked immunosorbent assay

The ELISA kit utilizes a double-antibody sandwich method to measure the level of the target indicator in the sample. A microtiter plate was coated with a purified capture antibody, and then the sample was added and incubated with an HRP-labeled detection antibody to form an antibody–antigen–enzyme-labeled antibody complex. The plate was washed thoroughly and TMB was added for color development. The absorbance was read at 450 nm using a microplate reader and the sample content was calculated using a standard curve.

Si-RNA transfection and plasmid transfection

The effective siRNA for HIF 1α and control siRNA were obtained from RiboBio Biotechnology (Shenzhen, Guangdong, China). When the cells reached 60%–70% confluence, the chondrocytes were transfected with HIF 1α siRNA using Lipofectamine 3000 siRNA transfection reagent (Thermo Fisher, UT, USA) according to the manufacturer's protocol. HIF 1α primers were designed according to the NCBI gene primer bank. The HIF 1α overexpression plasmid was constructed by RiboBio Biotechnology (Shenzhen, Guangdong, China). Chondrocytes were seeded in 6-well plates and then transfected with the LV003-HIF 1α plasmid using Lipofectamine 3000 (Invitrogen, California, USA) according to the manufacturer's protocol. Cells were transfected for 48 hours and then used for subsequent experiments.

Downloaded from academic.oup.com/burnstrauma/article/doi/10.1093/burnst/tkaf073/8315826 by guest on 12 October 2026

Table 1. Primer sequences used for qPCR

Primer	Sequence (5′ to 3′)
Forward HIF1alpha	ACCTTCATCGGAAACTCCAAAG
Reverse HIF1alpha	ACTGTTAGGCTCAGGTGAACT
Forward beta actin	GAGTCCTACGACATCATCGCT
Reverse beta actin	CCGACATAGTTTGGGAAACAGT
Forward Col2a1	GGGAATGTCCTCTGCGATGAC
Reverse Col2a1	GAAGGGGATCTCGGGGTTG
Forward Col2a1 promoter1	CGAAGCAACAGAAAGGAGCA
Reverse Col2a1 promoter1	TGGAAGGCAGGTCTGGAAAA
Forward Col2a1 promoter2	CATGAGCAGATGGACGTTGT
Reverse Col2a1 promoter2	GATGGGTTAGGGAGGCTGTG
Forward Col2a1 promoter3	CTCAATTCAGCTCTCCAGTTCC
Reverse Col2a1 promoter3	TCTCTGTGTAGCCCTGGTTG

Intracellular/extracellular lactate measurement

Intracellular/extracellular lactate measurement: Lactate levels in chondrocyte lysates and culture medium supernatants were measured using a lactate assay kit (Catalog #K627, BioVision, USA). Chondrocytes were seeded in 6-well plates at a density of 1×10^6 per well and incubated for 24 hours. Lactate was oxidized with lactate dehydrogenase and a colored product that bound to the probe was produced according to the kit protocol. The absorbance of the samples was read at 450 nm and the relative concentration of lactate was calculated from the standard curve.

qPCR analysis

Total RNA of chondrocytes was extracted with TRIzol, chloroform, and isopropanol. Complementary DNA (cDNA) was synthesized from total RNA using PrimeScriptTM RT Master Mix (Takara, Kusatsu, Japan) and amplified using SYBR Premix Ex TaqTM (Takara, Kusatsu, Japan). The expression levels of the target genes were quantified relative to β-actin levels using the $2^{-\Delta\Delta Ct}$ method. Each experiment was performed in triplicate and repeated three times independently. The forward and reverse primer sequences of all genes are listed in Table 1.

Measurement of intracellular ATP

Intracellular ATP content was measured using a test kit (Beyotime, S0027). The supernatant of the chondrocyte lysate was mixed with the ATP assay working solution and the relative intracellular ATP content was calculated by detecting the fluorescence intensity at 488 nm on a fluorescent microreader.

Measurement of the NAD: NADH ratio and NADP

NADPH ratio in chondrocytes: An NAD: NADH assay kit (S0175, Beyotime, China) was used to measure the NAD: NADH ratio. Ethanol was oxidized by ethanol dehydrogenase to form acetaldehyde, and NAD^+ was reduced to NADH. The resulting NADH reduced the electron-coupled reagent 1-methoxy-5-methylphenazinium methyl sulfate (1-mPMS) to WST-8 to form the orange-yellow formazan. The maximum absorption peak was at ~450 nm. The amount of formazan produced in the reaction system was proportional to the total amount of NAD^+ and NADH in the sample. The NADP: NADPH ratio was measured using an NADP: NADPH assay kit (S0179, Beyotime, China). Glucose-6-phosphate (G6P) was oxidized by glucose-6-phosphate dehydrogenase (G6PDH) to form 6-phosphogluconate (6-PG), during which $NADP^+$ was reduced to NADPH. The resulting NADPH reduced the electron-coupled reagent 1-mPMS to WST-8 to form an orange yellow formazan with a maximum absorption peak at ~450 nm. The amount of formazan produced in the reaction system was proportional to the total amount of $NADP^+$/NADPH in the sample.

Quantification of ROS species

The treated chondrocytes were washed three times with PBS and digested with 0.25% EDTA-free trypsin. They were resuspended in serum-free medium with 10 μM DCFH-DA (S0033S, Beyotime, China) and incubated at 37°C for 20 min, with several pipette mixing. After centrifugation, the residual DCFH-DA reagent was washed off with serum-free medium. The ROS intensity was measured by flow cytometry and a microplate reader at 488 nm excitation wavelength, and photographed by confocal microscopy at the same wavelength.

Chromatin immunoprecipitation (ChIP)-qPCR

The DNA and protein in the chondrocytes were cross-linked with 1% formaldehyde for 10 min at room temperature and quenched with 125 mM glycine for 5 min. The fixed cells were resuspended in lysis buffer (1% SDS, 5 mM EDTA, and 50 mM Tris–HCl, pH 8.1) with protease inhibitors, and the samples were sonicated for 30 cycles (30 s on and 30 s off) to fragment the chromatin into 150–900 bp pieces. The tubes were placed on a magnetic separation rack to precipitate the protein G magnetic beads in each immunoprecipitation sample. The supernatant was removed and the beads were washed three times with low salt buffer. The chromatin was eluted from the antibody/protein G magnetic beads and decrosslinked with 5 M NaCl and 2 μl proteinase K. The DNA was purified and qPCR experiments were performed. The primer sequences of the promoter of the collagen II gene for qPCR are listed in Table 1.

Micro-CT analysis

After 4 weeks of treatment, the mice were deep anesthetized and sacrificed by cervical dislocation, and the femur and tibia of the mice containing the intact knee joint were fixed with 4% paraformaldehyde in the functional position for 24 hours. Then, micro-CT scanning of the articular bone, subchondral bone, and trabeculae was performed at 65 kV and 144 μA. The complete images were preserved and CT analysis software was used to reconstruct and analyze the data on the subchondral bone and trabeculae of the tibial plateau.

Transmission electron microscopy

The chondrocytes were fixed overnight at 4°C in an electron microscope fixative, and then processed with 1% osmium fixation, dehydration, permeation, embedding, and ultrathin sectioning, and observed and photographed using a transmission electron microscope (Hitachi HT7800) at 0.5–2.0 million times magnification.

Data analysis

GraphPad Prism 9.3.1 software was used to determine the significance of differences in the experimental data. All data involving statistics are presented as mean ± S.D. One-way ANOVA followed by Dunnett's multiple comparison test was performed in experimental designs with one categorical independent variable (factor) and one continuous dependent

Downloaded from academic.oup.com/burnstrauma/article/doi/10.1093/burnst/tkaf073/8315826 by guest on 12 October 2026

variable. For example, in this study, the one-way ANOVA was conducted between the experimental group and the control group. Two-tailed Student's *t* test was performed to compare the two groups. A P value < 0.05 was considered significant and reflected in the statistical graph.

Results

Glycolytic lactate-dependent histone lactylation occurred in chondrocytes

Articular cartilage is an avascular, alymphatic tissue that relies on synovial fluid and subchondral bone for its nutrient supply [1]. In this unique environment, chondrocytes, the only cell type in articular cartilage, thrive in a hypoxic setting, with a resulting reliance on glycolysis rather than oxidative phosphorylation (OxPhos) to provide energy for their physiological functions [17]. In 6-well plates, 1×10^6 primary cardiomyocytes and primary chondrocytes were seeded per well and incubated for 24 hours. Compared with the primary cardiomyocyte cultures, the primary chondrocyte cultures exhibited higher concentrations of lactate in both the culture supernatant (0.009967 ± 0.001172 mM *vs* 0.004567 ± 0.0009292 mM, $P < 0.01$) and the cell lysate (0.1636 ± 0.005647 mM *vs* 0.04463 ± 0.001818 mM, $P < 0.0001$) (Figure S1a).

Given this reliance on the glycolytic energy supply in chondrocytes and the elevated concentrations of intra- and extracellular lactate, lactylation was explored. First, we found that the intracellular lactate content, lactylation level, and acetylation level were significantly reduced in response to treatment with graded concentrations of the glycolysis inhibitor 2-deoxy-D-glucose (2-DG) (Figure 1a, Figure S1b). Furthermore, in another experiment, oxamate and FX-11 were applied to selectively inhibit intracellular lactate dehydrogenase (LDH) activity to decrease the conversion of pyruvate to lactate. This treatment led to decreased lactylation accompanied by a reduction in the intracellular lactate content, whereas the total lysine acetylation (pan Kac) level remained unaffected (Figure 1b, c; Figure S1c, d). To further verify the correlation between intracellular lactylation and the lactate content, 5 mM 2-DG was applied to block intracellular glycolytic lactate production and graded concentrations of lactate were added to the medium, and the cells were incubated for 24 hours. As anticipated, the intracellular lactate content increased in parallel with the added concentration of lactate, resulting in a subsequent increase in total intracellular lysine lactylation (pan Kla) (Figure 1d, Figure S1e).

To identify the specific sites of lactylation in the chondrocytes, high-performance liquid chromatography–tandem mass spectrometry (HPLC–MS) analysis was performed after protein immunoprecipitation. The amino acid sequence was identified as the peptide YQKSTELLIR. According to the UniProt database, this peptide was derived from the mouse Histone H3 protein. The lysine at position 56 (average molecular weight, 128.1742 Da) exhibited a molecular weight shift of 71.9459 Da, which was very similar to the molecular weight of the group added during lactylation modification (72.021 Da), confirming that this lysine residue was modified by lactylation (Figure 1e). We then performed a pull-down assay in which magnetic beads coated with an anti-H3K56la antibody were added to the chondrocyte nuclear lysate to pull down the protein affected by H3K56 lactylation, and further western blot analyses were performed with the supernatant. The results showed that the lactylation level was significantly reduced after H3K56la was pulled down (Figure 1f, Figure S1f).

The glycolytic lactate/H3K56la/HIF 1α positive regulatory axis regulated collagen II synthesis

The production and modification of type II collagen in chondrocytes also rely on the normal expression of HIF 1α [18]. Abnormal expression of HIF 1α results in excessive modification of type II collagen, which causes a series of extracellular matrix-related diseases. Following the stimulation of chondrocytes with 10 mM lactate for 24 hours, mRNA sequencing was conducted prior to enrichment analysis of the differentially expressed genes. Compared with that in control group, the expression of the HIF 1α gene significantly increased in the lactate-stimulated chondrocytes. Gene Ontology analysis revealed enrichment of genes associated with cartilage development in chondrocytes. The enriched gene set was used to construct a heatmap based on the HIF 1α and Col2a1 genes (Figure 2a). Moreover, the addition of lactate to chondrocyte medium caused the upregulation of HIF 1α and Col2a1 gene expression, along with the occurrence of lactylation (Figure 2b). The occurrence of lactylation is regulated by the acetyltransferase CBP/P300 [19], and HIF 1α and Col2a1 gene expression decreased following treatment with the CBP/P300 inhibitor CBP/P300-IN-3 (Figure 2b). After genetic knockdown of HIF 1α, both Col2a1 gene expression and H3K56la decreased. Lactate addition was followed by increases in H3K56la and Col2a1 gene expression (Figure 2c, e; Figure S1g, h). The overexpression of the HIF 1α gene via plasmid transfection increased HIF 1α and Col2a1 gene expression in chondrocytes, accompanied by an increase in H3K56 lactylation (Figure 2d, g).

Notably, the intracellular lactate level changed accordingly before and after knockdown or overexpression of HIF 1α, but the pyruvate level did not change significantly (Figure 2f). These findings indirectly suggest that lactate dehydrogenase A (LDHA), which catalyses the conversion of pyruvate to lactate [20], may be the target of HIF 1α. Additionally, the introduction of the LDHA-specific inhibitor FX-11 to the medium of chondrocytes overexpressing HIF 1α led to reduced levels of lactylation and Col2a1 gene expression (Figure 2g; Figure S1i, j). Furthermore, the binding interaction between HIF 1α and LDHA was confirmed by a coimmunoprecipitation (co-IP) assay (Figure 2h). Taken together, the results of the above induction/blockade and knockdown/overexpression experiments suggest that a glycolytic lactate/H3K56la/HIF 1α regulatory axis exists in chondrocytes. Chromatin immunoprecipitation assays were performed to further explore the mechanisms underlying the regulation of Col2a1 by HIF 1α. The findings demonstrated that the transcription factor HIF 1α plays a regulatory role in collagen II synthesis by binding to the promoter of the Col2a1 gene (Figure 2i).

Addition of αKG altered the redox state in chondrocytes

PTOA results primarily from abnormal mechanical stimulation in articular cartilage, placing chondrocytes under oxidative stress. This state, in turn, leads to chondrocyte senescence

Downloaded from academic.oup.com/burnstrauma/article/doi/10.1093/burnst/tkaf073/8315826 by guest on 12 October 2026

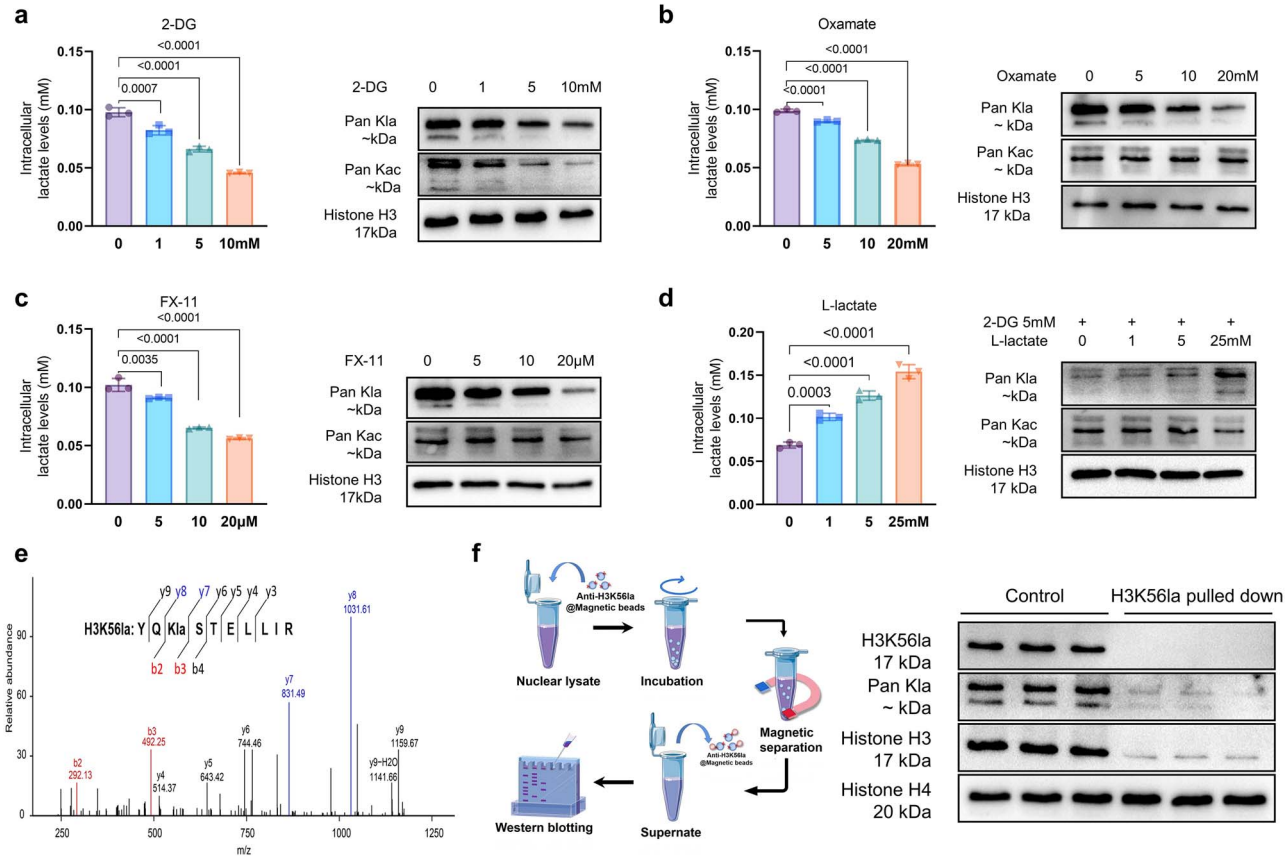


Figure 1. Glycolytic lactate-dependent histone lactylation occurs in chondrocytes. (**a**) Intracellular lactate levels and western blots results in chondrocytes after glycolysis inhibition by 2-DG. (**b**) Intracellular lactate levels and western blots results in chondrocytes after LDH inhibition by oxamate. (**c**) Intracellular lactate levels and western blots results in chondrocytes after LDHA inhibition by FX-11. (**d**) Intracellular lactate levels and western blots results in chondrocytes after 2-DG and lactate treatment. (**e**) Identification of lactylation sites by mass spectrometry. (**f**) Schematic diagram of pull-down experiment and western blots results before and after H3K56la pull-down. Significance was determined by one-way ANOVA with Dunnett's multiple comparison test (a-d). Images and measurements are representative of pooled data from at least three western blots or independent experiments. Data are presented as mean ± SD. *2-DG* 2-deoxy-D-glucose, *LDH* lactate dehydrogenase, *LDHA* lactate dehydrogenase A, *H3K56la* histone H3 lysine 56 lactylation

and apoptosis, further driving the progression of osteoarthritis—a vicious cycle in its development [21, 22]. It has also been reported that the intra- and extracellular lactate shuttles may be dependent on the intra- and extracellular redox gradients [23, 24]. On the basis of these two theories and the results of the above experiments, we postulated that modulating the intracellular redox status of chondrocytes to promote the shuttling of lactate into the cells and activate the glycolytic lactate/H3K56la/HIF 1α positive regulatory axis to further promote type II collagen synthesis could be a potential intervention and treatment strategy for osteoarthritis, particularly in the context of posttraumatic joint degeneration, where early intervention may prevent progression from acute injury to chronic degenerative disease.

αKG (1 mM and 2 mM) was added to the primary chondrocyte culture system, and the cells were incubated for 24 hours. The culture supernatant and cell lysate were collected for ELISA. The tricarboxylic acid cycle in αKG-treated chondrocytes was disrupted, as evidenced by the increases in the levels of intracellular acetyl-CoA (156.4 ± 6.756 ng/ml and 171.2 ± 2.174 ng/ml), succinyl-CoA(49.21 ± 2.233 ng/ml and 44.66 ± 3.158 ng/ml), and αKG dehydrogenase(2779 ± 415.2 ng/ml and 2538 ± 26.30 ng/ml) compared with those in the *tert*-butyl hydroperoxide (TBHP)-induced oxidative stress group. ATP production was not significantly altered (Figure 3a). Encouragingly, the intracellular reducing equivalents of NADH (7.887 ± 0.09452 μM (1 mM αKG) and 7.900 ± 0.1136 μM (2 mM αKG) *vs* 0.6633 ± 0.2706 μM (TBHP-induced oxidative stress), $P < 0.0001$) and NADPH (18.58 ± 0.2957 μM and 18.76 ± 0.5299 μM *vs* 5.597 ± 0.2957 μM, $P < 0.0001$) were significantly increased in the αKG-treated chondrocytes (Figure 3b, c), indicating that the cells were in a relatively reduced state. Furthermore, TBHP was applied to induce oxidative stress in chondrocytes prior to αKG treatment. This resulted in a substantial increase in intracellular ROS levels, as demonstrated by measurement with a fluorescence microplate reader and flow cytometric analysis. Notably, αKG treatment led to a reduction in intracellular ROS levels (Figure 3d–f). These results indicate that αKG may protect chondrocytes from damage caused by oxidative stress. In addition, transmission electron microscopy revealed consistent results: αKG alleviated TBHP-induced mitochondrial swelling, vacuolization and rupture of cristae within the chondrocytes (Figure S2).

The relative intracellular reduced state induced by αKG addition protected chondrocytes from oxidative stress damage

In our further study, flow cytometric analysis revealed a markedly higher apoptosis rate in oxidatively stressed chondrocytes than in their normal counterparts. Notably, after

Downloaded from academic.oup.com/burnstrauma/article/doi/10.1093/burnst/tkaf073/8315826 by guest on 12 October 2026

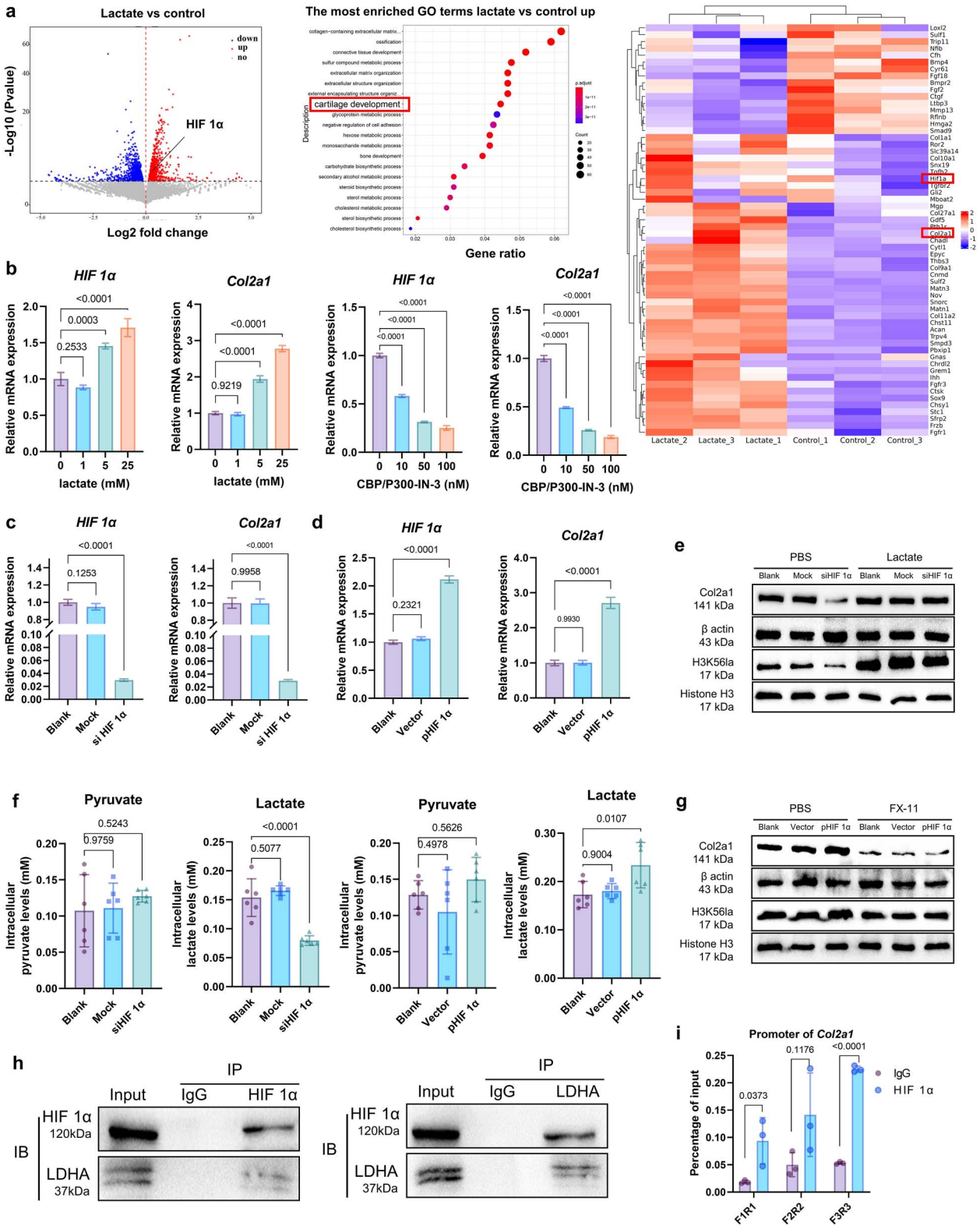


Figure 2. The glycolytic lactate/H3K56la/HIF 1α axis positively regulates collagen II synthesis by binding HIF 1α to the Col2a1 gene promoter. (**a**) Volcano plot, bubble plot of GO enrichment analysis and heat map of GO enriched gene set of RNA sequencing of chondrocytes before and after lactate treatment. (**b**) HIF 1α and Col2a1 expression after lactate or CBP/P300-IN-3 treatment by qPCR. (**c**) HIF 1α and Col2a1 expression after HIF 1α knockdown by qPCR. (**d**) HIF 1α and Col2a1 expression after HIF 1α overexpression by qPCR. (**e**) Western blot results of HIF 1α knockdown and lactate addition. (**f**) Intracellular pyruvate and lactate levels of chondrocytes in knockdown and overexpression experiments. (**g**) Western blot results of HIF 1α overexpression and FX-11 addition. (**h**) Co-IP results of HIF 1α and LDHA binding. (**i**) ChIP-qPCR results of chondrocytes. (b–d) Representative qPCR results of triplicate independent experiments. Significance was determined by one-way ANOVA with Dunnett's multiple comparison test (b–d, f) or by two-tailed Student's *t* test (i). Images and measurements are representative of pooled data from at least three western blots (**e, g, h**, and **i**) or independent experiments (b-d, f). Data are presented as mean ± SD. *HIF 1α* hypoxia-inducible factor-1 alpha, *Col2a1* collagen type II alpha 1 chain

Downloaded from academic.oup.com/burnstrauma/article/doi/10.1093/burnst/tkaf073/8315826 by guest on 12 October 2026

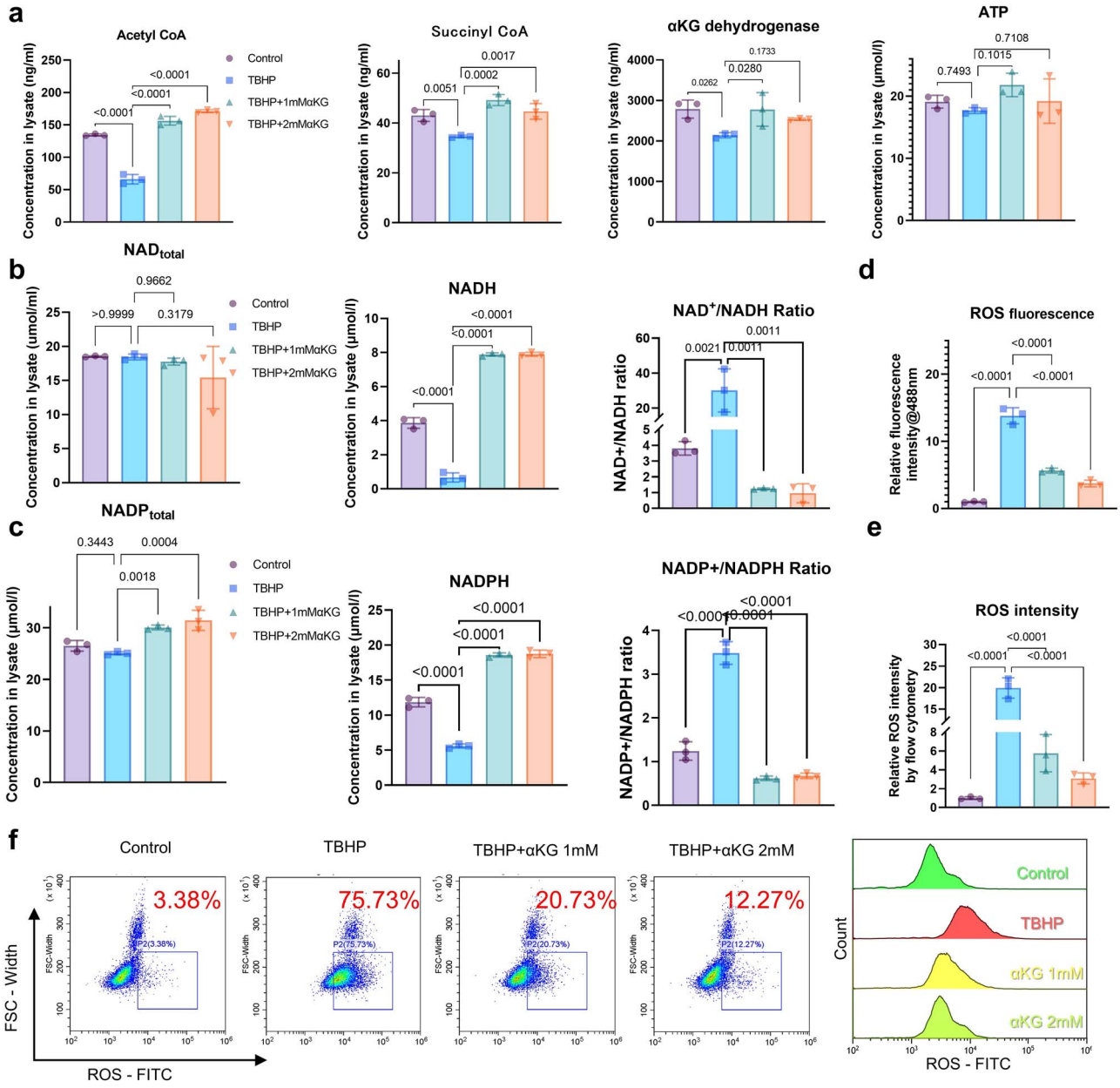


Figure 3. The addition of αKG alters the redox state in chondrocytes. (**a**) Acetyl CoA, succinyl CoA, αKG dehydrogenase, and ATP levels by ELISA in chondrocytes before and after TBHP treatment with or without αKG treatment. (**b**) NAD, NADH levels, and NAD$^+$/NADH ratio in chondrocytes before and after TBHP treatment with or without αKG treatment. (**c**) NADP, NADPH levels, and NADP$^+$/NADPH ratio in chondrocytes before and after TBHP treatment with or without αKG treatment. (**d**) Relative ROS levels by fluorescent microplate reader in chondrocytes before and after TBHP treatment with or without αKG treatment. (**e**) Flow cytometry relative ROS levels in chondrocytes before and after TBHP treatment with or without αKG treatment. (**f**) Flow cytometry scatter plot and count histograms of ROS levels in chondrocytes before and after TBHP treatment with or without αKG treatment. Significance was determined by one-way ANOVA with Dunnett's multiple comparison test (a-e). Images and measurements are representative of pooled data from at least three flow cytometry measurements (e and f) or independent experiments (a-d). Data are presented as mean ± SD. *αKG* alpha-ketoglutarate, *NADH* nicotinamide adenine dinucleotide, *NADPH* reduced nicotinamide adenine dinucleotide phosphate, *ROS* reactive oxygen species, *TBHP* tert-butyl hydroperoxide

6 hours of oxidative stress followed by 24 hours of αKG supplementation, some chondrocytes displayed markers of apoptosis, albeit at a significantly lower rate than the chondrocytes in the oxidatively stressed group did (5.183 ± 0.5601%, 5.335 ± 0.6576%, 5.920 ± 0.7169%, and 4.697 ± 0.4474% *vs* 14.57 ± 2.968%, $P < 0.001$) (Figure 4a–c). Subsequent western blot analysis of chondrocyte nuclear proteins revealed that compared with that in the control group, the level of lactylation in the nucleus of oxidatively stressed chondrocytes was significantly decreased, although lactylation was restored after αKG treatment (Figure 4d, Figure S1k). The relatively reduced intracellular state favours the shuttling of lactate into chondrocytes (Figure 4e).

We screened the GEO database (GSE148159) for protein markers that are characteristically altered under pathophysiological conditions in chondrocytes [25], including the matrix synthesis-related proteins aggrecan (ACAN) and Col2a1 as well as the matrix degradation-related proteins matrix metalloproteinase 13 (MMP13) and A Disintegrin and Metalloproteinase with Thrombospondin motifs 5 (ADAMTS5).

Downloaded from academic.oup.com/burnstrauma/article/doi/10.1093/burnst/tkaf073/8315826 by guest on 12 October 2026

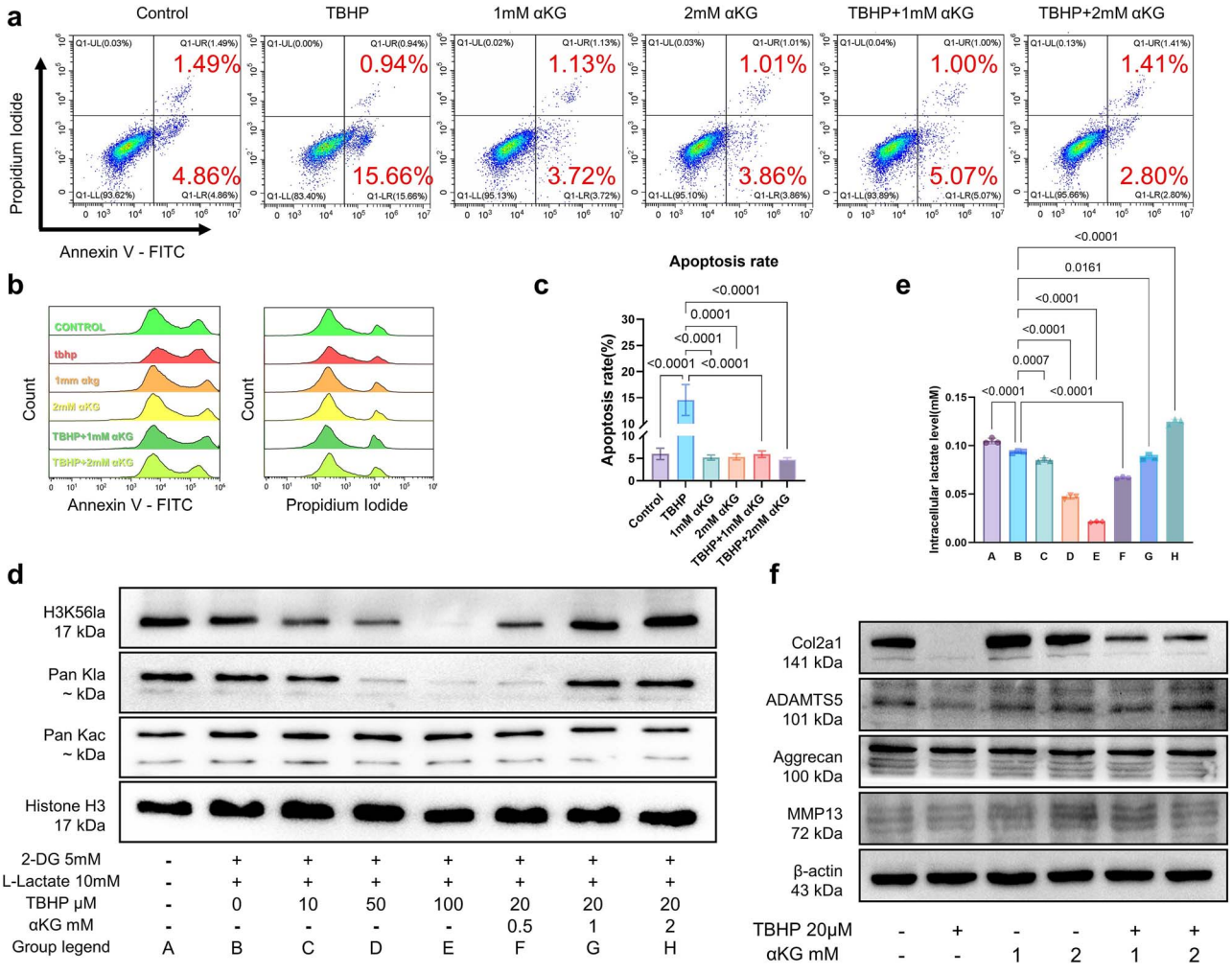


Figure 4. The intracellular relative reductive state promotes lactate shuttling into chondrocytes to activate H3K56la and protects chondrocytes from apoptosis. (**a**) Flow cytometry of apoptotic chondrocytes under oxidative stress and reductive protection. (**b**) Flow cytometry count histograms of apoptotic chondrocytes. (**c**) Apoptosis rate of chondrocytes. (**d**) Western blot results of oxidative stress and reductive protection markers in chondrocytes. (**e**) Intracellular lactate levels in chondrocytes under oxidative stress and reductive protection. (**f**) Western blot results of oxidative-stressed and reductive-protected chondrocytes. Significance was determined by one-way ANOVA with Dunnett's multiple comparison test (c and e). Images and measurements are representative of pooled data from at least three flow cytometry measurements (a and b), western blots (d and f), or independent experiments (e). Data are presented as mean ± SD *H3K56la* histone H3 lysine 56 lactylation

We performed western blot analysis and found that Col2a1 synthesis was significantly inhibited in oxidatively stressed chondrocytes and that this effect was alleviated by αKG treatment (Figure 4f, Figure S1l).

In summary, it can be concluded that the relatively reduced intracellular state was beneficial for the survival of chondrocytes. This beneficial effect was primarily due to the decrease in the intracellular ROS content, the promotion of lactate shuttling into the cell, the activation of the intracellular glycolytic lactate/H3K56la/HIF 1α regulatory axis in chondrocytes resulting from the relatively reduced state, and the subsequent promotion of type II collagen synthesis in chondrocytes. These mechanisms collectively protect chondrocytes from damage induced by oxidative stress.

αKG alleviated osteoarthritis by promoting H3K56 lactylation and HIF 1α expression

As ACL injuries account for ~25% of PTOA cases in young athletes [26], we employed ACLT method in C57BL/6 mice to simulate the pathological state of cartilage subjected to abnormal mechanical stress. Twenty mice of the same age on the same genetic background were selected. A total of 15 mice were randomly assigned to three experimental groups after undergoing ACLT, while the mice in the control group, containing five mice, underwent a sham operation in which the joint cavity was cut apart but the ACL remained intact. The mice in the αKG treatment group were treated with 0.25% and 0.75% αKG in their drinking water.

All the mice were sacrificed by cervical dislocation under deep anaesthesia 4 weeks after the operation. The immunofluorescence staining results confirmed the chondroprotective effect of HIF 1α and H3K56la. HIF 1α expression and H3K56la were reduced in the mice in the ACLT osteoarthritis model, whereas αKG treatment was accompanied by the restoration of HIF 1α expression (relative fluorescence intensity 0.8166 ± 0.1823 in the low-αKG treatment group *vs* 0.4064 ± 0.1175 in the OA group, $P = 0.0035 < 0.01$) and H3K56la (relative fluorescence intensity 0.9823 ± 0.1255 and 0.8456 ± 0.08477 *vs* 0.4429 ± 0.2403, $P < 0.01$) (Figure 5a).

Before the knee specimens were sectioned for analysis, μCT analysis was performed. The number of osteophytes in the

Downloaded from academic.oup.com/burnstrauma/article/doi/10.1093/burnst/tkaf073/8315826 by guest on 12 October 2026

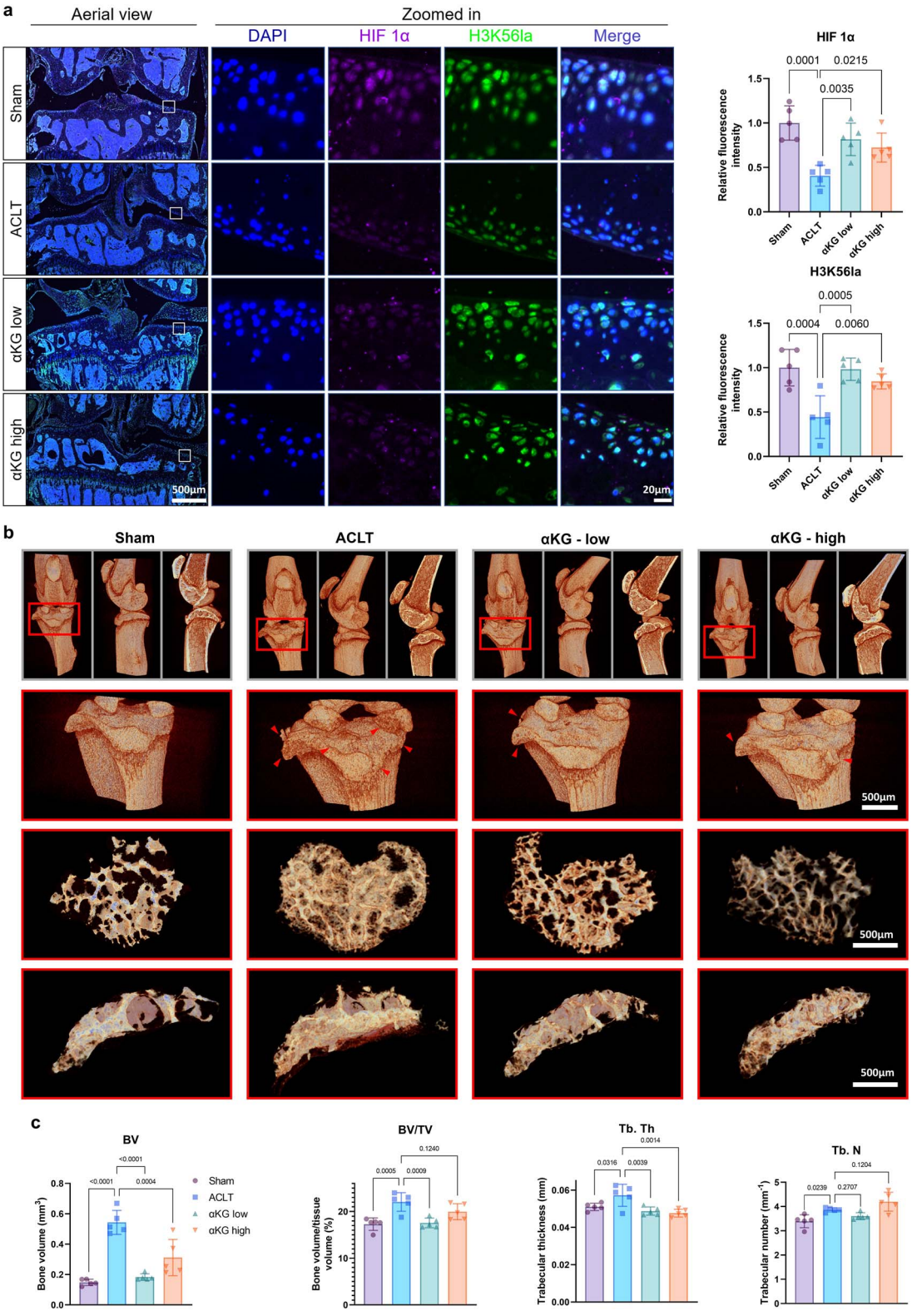


Figure 5. H3K56 lactylation in chondrocytes alleviates osteophyte formation and subchondral osteosclerosis in osteoarthritis. (**a**) Immunofluorescence of HIF 1α and H3K56la in chondrocytes (scale bar = 500 μm in aerial view, 20 μm in zoomed images) and relative fluorescence intensity of HIF 1α and H3K56la. (**b**) 3D micro-CT reconstruction of right knee joints of mice (red arrow indicates osteophytes, scale bar = 500 μm, n = 5). (**c**) Bone volume, bone volume/tissue volume, trabecular thickness, and trabecular number of subchondral bone. Significance was determined by one-way ANOVA with Dunnett's multiple comparison test (a, c). Data are mean ± SD from at least five experiments. *HIF 1α* hypoxia-inducible factor-1 alpha, *H3K56la* histone H3 lysine 56 lactylation

Downloaded from academic.oup.com/burnstrauma/article/doi/10.1093/burnst/tkaf073/8315826 by guest on 12 October 2026

ACLT group was significantly greater than that in the control group, and the number of osteophytes in the αKG treatment group was between that in the disease group and that in the control group (Figure 5b). The subchondral bone of the tibial plateau was selected as the region of interest (ROI) for quantitative analysis. Compared with the normal group, the disease model group had a significantly greater bone volume (BV) and bone volume/total volume ratio (BV/TV) and greater trabecular thickness (Tb. Th) in the subchondral bone of the knee. However, there was no significant difference in trabecular number. Osteophyte formation and subchondral bone sclerosis were alleviated to some degree in the αKG treatment group (Figure 5c).

Immunohistochemical (IHC) staining of the sections revealed that Col2a1 expression in the knee cartilage of mice in the disease model group was reduced. Moreover, compared with those in the control group and the αKG treatment group, the levels of MMP13 and ADAMTS5 were increased (Figure 6a, b). Further assessments through HE, safranin O, and toluidine blue staining, along with quantitative analyses of changes in articular cartilage, were carried out (Figure 7a). The number of chondrocytes in the articular cartilage of the mice was significantly lower in the osteoarthritis group than in the control and αKG treatment groups (Figure 7b). Additionally, the thickness of the articular cartilage was reduced. The thickness of the calcified cartilage was increased (Figure 7c, d). The OARSI score was significantly higher in the osteoarthritis group than in the control and αKG treatment groups (Figure 7e). These findings indicate that αKG treatment alleviates osteoarthritis.

Discussion

Mammalian cells typically function in a normoxic environment. It is generally believed that glycolysis may occur only in hypoxic environments [27, 28]. Since the discovery of the Warburg effect and the increase in studies on tumour cells and immune cells, glycolysis has gradually been recognized as a crucial process of glucose metabolism and energy supply [29, 30]. Lactate produced via glycolysis in mammalian cells is increasingly recognized not only as a substrate for gluconeogenesis but also as a potential intracellular signal involved in the regulation of intracellular gene expression and physiological functions [31]. Under physiological conditions, mammals maintain low intracellular and blood pyruvate concentrations, whereas lactate levels increase dramatically during exercise, especially intense anaerobic exercise. In chondrocytes, local pyruvate and lactate levels are higher in cartilage than in blood, probably because of the glycolytic activity, and because of this physiological feature, the study of lactylation modifications in chondrocytes is of interest [32].

Intracellular lactate is generated through a reaction involving pyruvate and NADH catalysed by LDHA [33]. A recent study showed that the induction of intracellular NADPH production in mouse chondrocytes significantly alleviates articular cartilage degeneration [34]. Our data demonstrate that αKG-induced reductive stress (as evidenced by the elevated NADPH and NADH levels; Figure 3b–c) promotes extracellular lactate influx into chondrocytes (Figure 4e), subsequently increasing H3K56 lactylation and collagen synthesis. This phenomenon is consistent with Brooks' lactate shuttle theory [23], which posits that lactate serves as a redox-coupled metabolite whose transmembrane transport is dynamically regulated by the cellular energy state. Importantly, monocarboxylate transporters (MCTs)—particularly MCT1 (influx) and MCT4 (efflux)—exhibit redox-sensitive gating properties. Under reducing conditions (e.g. high NADPH levels), MCT1 undergoes conformational changes that favour lactate influx, while MCT4 activity is suppressed to limit lactate efflux [35]. Therefore, NADH and NADPH alter the intracellular redox state and promote lactate shuttling into the cell. This results in increased lactylation in the chondrocyte nucleus. α-Ketoglutarate acts as a lactate trap in chondrocytes, inducing the shuttling of lactate into the cell and then capturing it, tightly binding it to histones via lactylation to support physiological function.

Among the three spin isomers of lactate (D-, L-, and DL-lactate), L-lactate is the predominant isomer formed in mammalian cells via glycolysis [36]. Consequently, we used an L-lactate assay kit to measure the intra- and extracellular lactate contents. Previous experiments revealed that L-lactate directly promotes lactylation of specific lysine residues on histones. In contrast, lysine lactylation mediated by D-lactate (K(D-la)) occurs only in cytosolic proteins in close contact with lactylglutathione (LGSH) [37]. In the present experiments, L-lactate, D-lactate, and DL-lactate were added to the chondrocyte medium; however, only the addition of L-lactate promoted the occurrence of histone lactylation in chondrocytes. On the basis of the above studies, all the lactylation modifications studied herein, particularly histone lysine lactylation, refer to the L-lactylation modification induced by L-lactate.

Through HPLC–MS analysis, we precisely identified the lysine (K) residue in the peptide sequence corresponding to the 57th amino acid of Histone H3. Considering the methionine (M) translated by the start codon AUG as the initiation point and excluding it from the ordinal number of amino acids, we confirmed that the identified lysine is the 56th amino acid on Histone H3. In addition, the molecular weight of lysine calculated according to the molecular formula $C_6H_{14}N_2O_2$ is 146 Da, while the average molecular weights of amino acids after dehydration synthesis are reduced by ∼18 Da, and there may be isotopic molecules under the actual conditions. The average molecular weight of the lysine in the identified peptide was 128.1742 Da; similarly, the average molecular weight of the lactyl group was 72.02113 Da.

Posttranslational modifications of proteins in mammalian cells vary spatially and temporally across cell states. This study confirmed that H3K56 is the main site of lactylation in the nucleus of chondrocytes. However, whether other modification sites are present in chondrocytes and how these modification sites are related to each other need to be further explored.

HDACs function as lactylation erasers [37], but they lack specificity because they are also methylation and acetylation erasers [38, 39]. Therefore, adding HDACs to chondrocytes for inhibition of lactylation inadvertently affects other acylation modifications, including methylation and acetylation. This broad impact could cloud the interpretability of the results. To specifically inhibit lactylation modifications, we employed the LDHA-specific inhibitor FX-11 and conducted knockdown experiments on HIF 1α. These targeted interventions, combined with other experiments, elucidated the physiological relevance of lactylation in chondrocytes. Notably, the current study has definite methodological limitations. Specifically, site-directed mutagenesis of K56 is needed in future investigations to conclusively elucidate the regulatory mechanism of H3K56la. Regrettably, such experiments were

Downloaded from academic.oup.com/burnstrauma/article/doi/10.1093/burnst/tkaf073/8315826 by guest on 12 October 2026

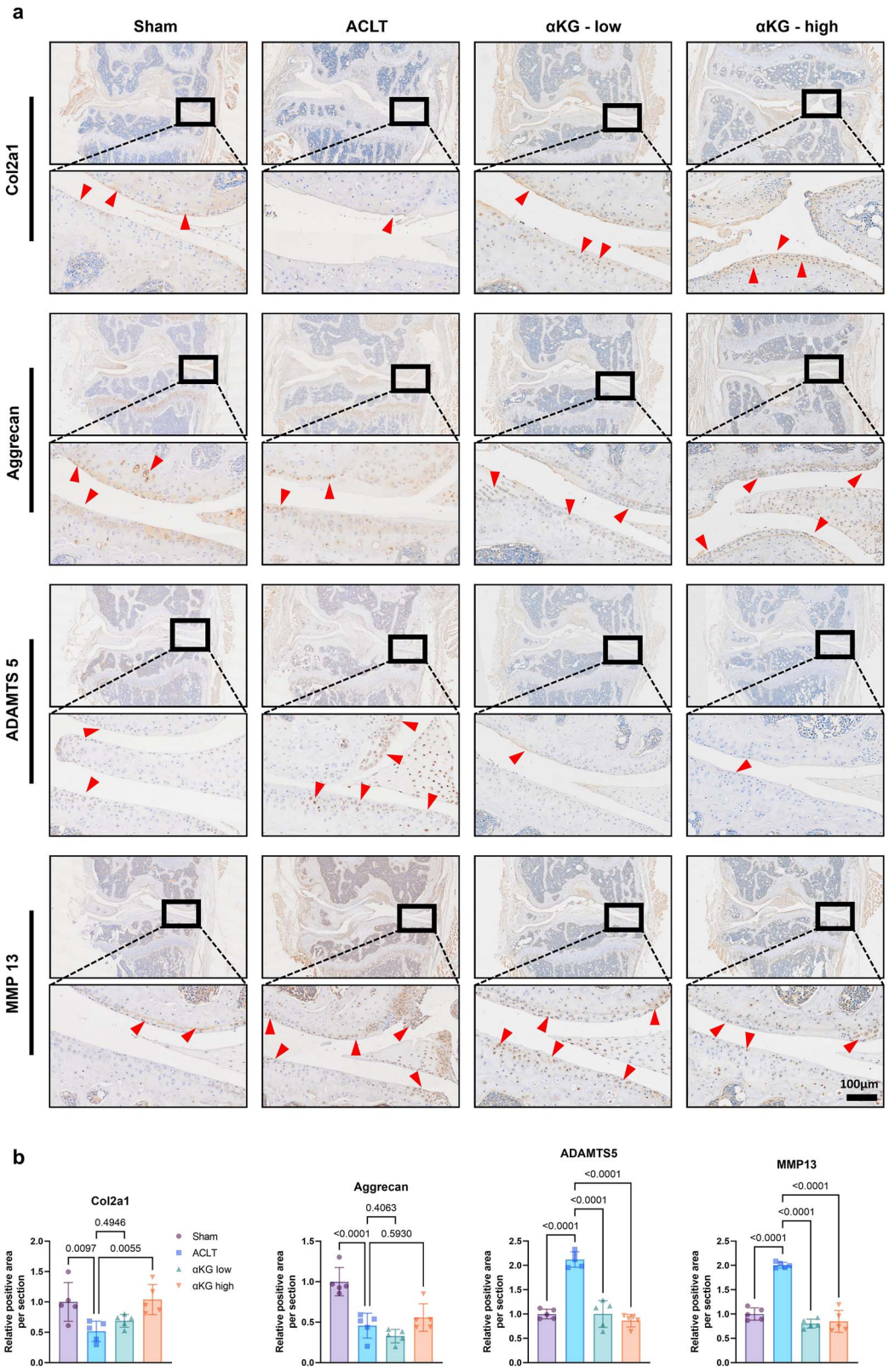


Figure 6. H3K56 lactylation in chondrocytes preserves cartilage matrix in mouse knee joints. (**a**) Immunohistochemistry of Col2a1, aggrecan, ADAMTS5, and MMP 13 in mouse knee joint (red arrow indicates the typically positive area, scale bar = 100 μm, n = 5). (**b**) Relative positive area of Col2a1, aggrecan, ADAMTS5, and MMP 13 per section. Significance was determined by one-way ANOVA with Dunnett's multiple comparison test (b). Data are mean ± SD from at least five experiments. *ADAMTS5* a Disintegrin and Metalloproteinase with Thrombospondin motifs 5, *MMP 13* matrix metalloproteinase 13, *H3K56la* histone H3 lysine 56 lactylation

Downloaded from academic.oup.com/burnstrauma/article/doi/10.1093/burnst/tkaf073/8315826 by guest on 12 October 2026

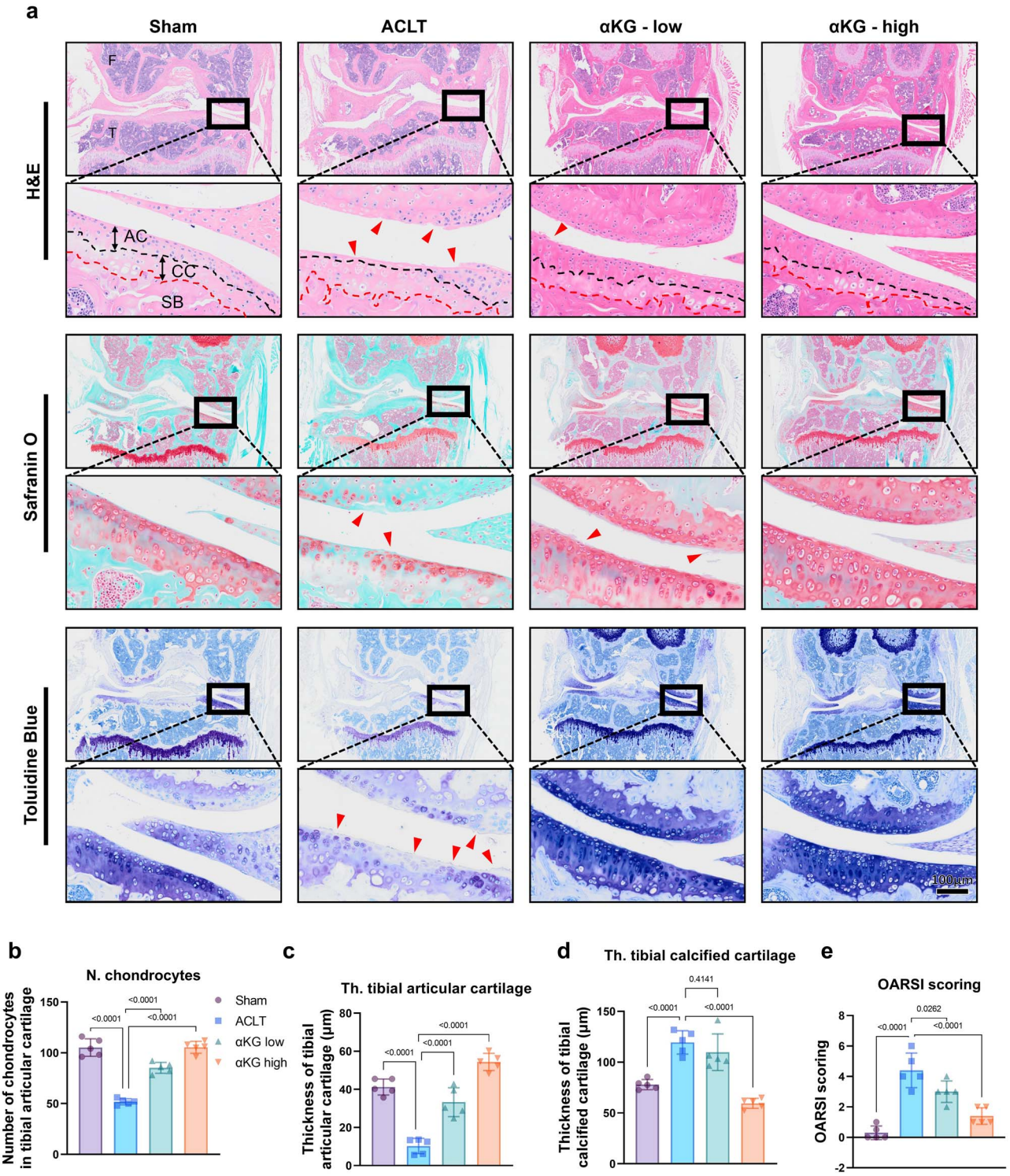


Figure 7. H3K56 lactylation in chondrocytes attenuates cartilage erosion in mouse knee joints. (**a**) H&E, safranin O, and toluidine blue staining of mouse knee joints (red arrow indicates cartilage erosion. Scale bar = 100 μm, n = 5). Chondrocyte number (**b**), thickness (**c**), calcified cartilage thickness (**d**), and OARSI score (**e**) of tibial articular cartilage. (e) OARSI scoring of mouse specimens. Significance was determined by one-way ANOVA with Dunnett's multiple comparison test (b-e). Data are mean ± SD from at least five experiments. *F* femur, *T* tibia, *AC* articular cartilage, *CC* calcified cartilage, *SB* subchondral bone

not feasible under our current technological constraints. Furthermore, the clinical relevance of these findings could be substantially increased through subsequent studies incorporating human osteoarthritis-derived articular cartilage specimens, particularly those obtained during arthroplasty procedures at different disease stages.

Our study demonstrated that exposure to high concentrations of lactate—exceeding physiological levels—induced detachment, inhibited growth, and, in severe cases, led to the death of chondrocytes. In contrast, a low-lactate environment, with lactate concentrations similar to those found under physiological conditions, was favorable for the lactylation of

Downloaded from academic.oup.com/burnstrauma/article/doi/10.1093/burnst/tkaf073/8315826 by guest on 12 October 2026

H3K56 in chondrocytes and facilitated the expression of the transcription factor HIF 1α. HIF 1α, in turn, promoted the synthesis of type II collagen by binding to the promoter region of the Col2a1 gene. These findings indicate that varying concentrations of lactate can produce distinct biological effects depending on the cellular state. Furthermore, the transport of lactate into and out of chondrocytes is regulated by the intracellular and extracellular redox gradient. This relationship offers a novel perspective for artificially modulating glycolytic lactate transport within chondrocytes. Compared to the exogenous addition of lactate, such an intervention strategy avoids the complications associated with high lactate concentrations and the challenges of controlling its regulatory outcomes.

The protective mechanism of H3K56la in articular cartilage extended beyond the activation of the glycolytic lactate/H3K56la/HIF 1α positive regulatory axis, which primarily governs collagen II synthesis. In addition, H3K56la alleviated chondrocyte apoptosis. As discussed in previous studies, HIF 1α also regulates the expression of BMP2, Sox9, Runx2 and other genes [40]. These genes, including Runx2, are also involved in other bone-related diseases [41]. However, it can be concluded that the activation of this positive regulatory axis further promotes collagen II synthesis through the binding of the transcription factor HIF 1α to the Col2a1 gene promoter. Moreover, we observed the binding between HIF 1α and LDHA by co-IP, and the precise mechanism remains to be studied. A glycolytic lactate/H3K56la/HIF 1α positive feedback loop may exist in chondrocytes. Promoting the activation of this positive feedback loop is a potential protective strategy for osteoarthritic articular chondrocytes. This is one of the main goals of our future research.

Earlier studies suggested that lactylation might be a nonenzymatic reaction [42], and our current study confirmed that lactate accumulation and catalysis by the acetyltransferase P300 are integral events during the induction of lactylation, at least in primary mouse chondrocytes. It is not possible to simply assume that the accumulation of lactate is good or bad or to simply draw the conclusion that lactylation is friend or foe without considering the cell type and its pathophysiological state. It is certain that the production of lactate via glycolysis in mammalian cells inevitably alters intracellular acid–base homoeostasis and that the presence of lactate promotes lactylation to some extent. Therefore, lactate acts as a signalling molecule. Understanding how lactate further influences gene expression, posttranslational modifications, and cellular physiological activities requires further investigation. While the changes in the extracellular matrix (ECM) of cartilage associated with the pathogenesis of osteoarthritis are well understood, it is now increasingly clear that in many cases, the pathogenesis of the disease may initially be manifested in the region of the matrix that directly surrounds the chondrocytes, known as the pericellular matrix (PCM) [43]. The PCM acts as a key transducer or 'filter' for chondrocyte-derived biochemical and biomechanical signals, helping to regulate the homoeostatic balance of chondrocyte metabolic activity in response to environmental stimulus-related signals. Type II collagen is relatively specific to hyaline cartilage, and disruption of type II collagen is considered a potential biomarker for osteoarthritis. In other words, an imbalance between the synthesis and degradation of type II collagen, which causes chondrocyte destruction, may be important for the pathogenesis of osteoarthritis.

The roles of αKG as an antioxidant and in the alleviation of osteoarthritis has been reported several times [15, 44]. Unlike N-acetylcysteine (NAC), which directly scavenges ROS through thiol group donation, αKG participates in dual mechanisms by fundamentally altering the cellular redox architecture. Our data revealed that αKG increases the levels of NADH and NADPH, sustaining the antioxidant capacity. More importantly, αKG-mediated metabolic reprogramming facilitates lactate influx, unlike NAC, thereby coupling redox homoeostasis with epigenetic regulation. TBHP was applied to chondrocytes in an in vitro experiment to simulate intracellular oxidative stress. After screening via a CCK8 assay, a concentration of 20 μM was determined to produce a relatively oxidative state in chondrocytes. Stimulation with TBHP at this concentration did not fully mimic the osteoarthritic state of articular chondrocytes, which was not the original goal of the in vitro experiments. We performed these experiments to verify that altering the intracellular redox state affects the expression of Col2a1 in chondrocytes following lactate shuttling and the occurrence of lactylation. These findings lay the foundation for exploring strategies for chondrocyte protection and osteoarthritis therapy.

In contrast, in the *in vivo* experiments with ACLT models, in which articular chondrocytes were subjected to mechanical stress, a cascade of pathological changes related to chondrocyte destruction was inevitably triggered, involving pathophysiological processes such as oxidative stress and inflammation; thus, the origins of the pathological changes observed in the animal sections and other experimental indicators were not limited to alterations in Col2a1 expression. Therefore, in subsequent *in vivo* experiments, the expression of Col2a1 in particular chondrocytes was also regulated to a certain extent after the redox status of the chondrocytes was altered, and the indices associated with these pathological changes also changed accordingly, thus delaying the progression of osteoarthritis but not completely curing the disease or reversing all the pathological changes.

Conclusions

In this study, we investigated the interaction between histone lactylation and HIF 1α, uncovering that the glycolytic lactate/H3K56la/HIF 1α regulatory axis plays a positive regulatory role in the synthesis of type II collagen in chondrocytes. Our findings further demonstrated that this regulatory axis is activated through modulation of the intracellular redox environment within chondrocytes. This activation facilitates the transport of extracellular lactate into the cells, enhances the expression of the Col2a1 gene—which encodes type II collagen—and protects chondrocytes against apoptosis induced by oxidative stress. Moreover, *in vivo* experimental results showed that activation of this positive regulatory axis mitigated pathological changes associated with osteoarthritis in animal models. Collectively, our data indicate that a reduced intracellular redox state in chondrocytes promotes H3K56 lactylation and upregulates HIF 1α expression, thereby regulating type II collagen synthesis. These insights suggest that inducing such molecular changes may represent a promising therapeutic approach for the treatment of osteoarthritis.

Downloaded from academic.oup.com/burnstrauma/article/doi/10.1093/burnst/tkaf073/8315826 by guest on 12 October 2026

Abbreviations

2-DG, 2-deoxy-D-glucose; ac, acetylation; ACAN, aggrecan; ACL, anterior cruciate ligament; ADAMTS5, a Disintegrin and Metalloproteinase with Thrombospondin motifs 5; αKG, alpha-ketoglutarate; BV, bone volume; BV/TV, bone volume/total volume ratio; Col2a1, collagen type II alpha 1 chain; ECM, extracellular matrix; ELISA, enzyme-linked immunosorbent assay; H3K56, histone H3 lysine 56; HE, hematoxylin–eosin; HIF 1α, hypoxia-inducible factor-1 alpha; IHC, immunohistochemical; la, lactylation; LDH, lactate dehydrogenase; LDHA, lactate dehydrogenase A; LGSH, lactylglutathione; MCT, monocarboxylate transport; MMP 13, matrix metalloproteinase 13; NADH, nicotinamide adenine dinucleotide; NADPH, reduced nicotinamide adenine dinucleotide phosphate; OARSI, Osteoarthritis Research Society International; OxPhos, oxidative phosphorylation; Pan Kac, total lysine acetylation; Pan Kla, total lysine lactylation; PCM, pericellular matrix; PTOA, Post-traumatic osteoarthritis; qPCR, quantitative polymerase chain reaction; ROI, region of interest; ROS, reactive oxygen species; Tb. Th, trabecular thickness; TBHP, *tert*-butyl hydroperoxide; μCT, micro computerized tomography

Author contributions

Zicai Dong (Conceptualization, Data curation, Formal Analysis, Investigation, Methodology, Resources, Software, Visualization, Writing—original draft, Writing—review & editing), Di Liu (Investigation, Validation, Writing—original draft, Writing—review & editing), Guangyun Hu (Methodology), Zeyu Yang (Methodology), Qin Shu (Conceptualization, Methodology), Qijie Dai (Software, Visualization), Hao Tang (Methodology), Chuan Yang (Methodology), Chunrong Zhao (Methodology), Xiaoshan Gong (Methodology), Rujie Wang (Methodology), Weikai Kong (Methodology), and Shiwu Dong (Conceptualization, Funding acquisition, Project administration, Supervision)

Supplementary data

Supplementary data are available at *Burns & Trauma Journal* online.

Ethics approval

In the study, mice were purchased from the Laboratory Animal Center of Army Medical University (production license number: SCXK(yu)2022–0011). The study was approved by the animal ethics committee of Army Medical University (animal ethical statement number: AMUWEC20226055).

Conflict of interest

The authors declare no conflict of interest.

Funding

This work was supported by the Integration Project of NSFC Joint Fund for Regional Innovation and Development (U23A6008) and the National Nature Science Foundation of China (81930067).

Data availability

The data that support the findings of this study are available from the corresponding author upon reasonable request.

Declaration of AI and AI-assisted technologies application

The authors declare AI and AI-assisted technologies were not applied in this study at any stage, including the researching and writing process.

References

1. Bank NC, Sanghvi P, Hecht CJ, Mistovich RJ. The epidemiology of posttraumatic osteoarthritis of the knee in the United States: an analysis of 948,853 patients from 2000 to 2022. *J Am Acad Orthop Surg*. 2024;**32**:e313–20. https://doi.org/10.5435/JAAOS-D-23-00662.
2. Castano Betancourt MC, Maia CR, Munhoz M, Morais CL, Machado EG. A review of risk factors for post-traumatic hip and knee osteoarthritis following musculoskeletal injuries other than anterior cruciate ligament rupture. *Orthop Rev*. 2022;**14**:38747. https://doi.org/10.52965/001c.38747.
3. Galeazzi Y, Houel N, Gouaux L, Rohan A, Le Heiget H, Jung C, *et al.* Effect of osteopathic manipulative treatment on pain in palliative care patients: a randomized placebo-controlled clinical trial. *Pain Rep*. 2025;**10**:e1239. https://doi.org/10.1097/PR9.0000000000001239.
4. Mobasheri A, Platt N, Thorpe C, Shakibaei M. Regulation of 2-deoxy-D-glucose transport, lactate metabolism, and MMP-2 secretion by the hypoxia mimetic cobalt chloride in articular chondrocytes. *Ann N Y Acad Sci*. 2006;**1091**:83–93. https://doi.org/10.1196/annals.1378.057.
5. Huang YF, Wang G, Ding L, Bai ZR, Leng Y, Tian JW, *et al.* Lactate-upregulated NADPH-dependent NOX4 expression via HCAR1/PI3K pathway contributes to ROS-induced osteoarthritis chondrocyte damage. *Redox Biol*. 2023;**67**:102867. https://doi.org/10.1016/j.redox.2023.102867.
6. Xia J, Qiao Z, Hao X, Zhang Y. LDHA-induced histone lactylation mediates the development of osteoarthritis through regulating the transcription activity of TPI1 gene. *Autoimmunity*. 2024;**57**:2384889. https://doi.org/10.1080/08916934.2024.2384889.
7. Yang B, Li Z, Yang Z, Zhao P, Lin S, Wu J, *et al.* Recapitulating hypoxic metabolism in cartilaginous organoids via adaptive cell-matrix interactions enhances histone lactylation and cartilage regeneration. *Nat Commun*. 2025;**16**:2711. https://doi.org/10.1038/s41467-025-57779-6.
8. Duval E, Bouyoucef M, Leclercq S, Baugé C, Boumédiene K. Hypoxia inducible factor 1 alpha down-regulates type i collagen through Sp3 transcription factor in human chondrocytes. *IUBMB Life*. 2016;**68**:756–63. https://doi.org/10.1002/iub.1539.
9. Allen KD, Golightly YM, White DK. Gaps in appropriate use of treatment strategies in osteoarthritis. *Best Pract Res Clin Rheumatol*. 2017;**31**:746–59. https://doi.org/10.1016/j.berh.2018.05.003.
10. Watt FE, Corp N, Kingsbury SR, Frobell R, Englund M, Felson DT, *et al.* Towards prevention of post-traumatic osteoarthritis: report from an international expert working group on considerations for the design and conduct of interventional studies following acute knee injury. *Osteoarthr Cartil*. 2019;**27**:23–33. https://doi.org/10.1016/j.joca.2018.08.001.
11. Khella CM, Horvath JM, Asgarian R, Rolauffs B, Hart ML. Anti-inflammatory therapeutic approaches to prevent or delay post-traumatic osteoarthritis (PTOA) of the knee joint with a focus on sustained delivery approaches. *Int J Mol Sci*. 2021;**22**:8005. https://doi.org/10.3390/ijms22158005.
12. Anderson DD, Chubinskaya S, Guilak F, Martin JA, Oegema TR, Olson SA, *et al.* Post-traumatic osteoarthritis: improved understanding and opportunities for early intervention. *J Orthop Res Off Publ Orthop Res Soc*. 2011;**29**:802–9. https://doi.org/10.1002/jor.21359.
13. Ye X, Li X, Qiu J, Kuang Y, Hua B, Liu X. Alpha-ketoglutarate ameliorates age-related and surgery induced temporomandibular

Downloaded from academic.oup.com/burnstrauma/article/doi/10.1093/burnst/tkaf073/8315826 by guest on 12 October 2026

joint osteoarthritis via regulating IKK/NF-κB signaling. *Aging Cell*. 2024;**23**:e14269. https://doi.org/10.1111/acel.14269.
14. He R, Wei Y, Peng Z, Yang J, Zhou Z, Li A, *et al.* α-Ketoglutarate alleviates osteoarthritis by inhibiting ferroptosis via the ETV4/SLC7A11/GPX4 signaling pathway. *Cell Mol Biol Lett*. 2024;**29**:88. https://doi.org/10.1186/s11658-024-00605-6.
15. Liu L, Zhang W, Liu T, Tan Y, Chen C, Zhao J, *et al.* The physiological metabolite α-ketoglutarate ameliorates osteoarthritis by regulating mitophagy and oxidative stress. *Redox Biol*. 2023;**62**:102663. https://doi.org/10.1016/j.redox.2023.102663.
16. Wang X, Xue Y, Hao K, Peng B, Chen H, Liu H, *et al.* Sustained therapeutic effects of self-assembled hyaluronic acid nanoparticles loaded with α-ketoglutarate in various osteoarthritis stages. *Biomaterials*. 2025;**314**:122845. https://doi.org/10.1016/j.biomaterials.2024.122845.
17. Zheng L, Zhang Z, Sheng P, Mobasheri A. The role of metabolism in chondrocyte dysfunction and the progression of osteoarthritis. *Ageing Res Rev*. 2021;**66**:101249. https://doi.org/10.1016/j.arr.2020.101249.
18. Stegen S, Laperre K, Eelen G, Rinaldi G, Fraisl P, Torrekens S, *et al.* HIF-1α metabolically controls collagen synthesis and modification in chondrocytes. *Nature*. 2019;**565**:511–5. https://doi.org/10.1038/s41586-019-0874-3.
19. Zhang D, Tang Z, Huang H, Zhou G, Cui C, Weng Y, *et al.* Metabolic regulation of gene expression by histone lactylation. *Nature*. 2019;**574**:575–80. https://doi.org/10.1038/s41586-019-1678-1.
20. Doherty JR, Cleveland JL. Targeting lactate metabolism for cancer therapeutics. *J Clin Invest*. 2013;**123**:3685–92. https://doi.org/10.1172/JCI69741.
21. Dan Dunn J, Alvarez LA, Zhang X, Soldati T. Reactive oxygen species and mitochondria: a nexus of cellular homeostasis. *Redox Biol*. 2015;**6**:472–85. https://doi.org/10.1016/j.redox.2015.09.005.
22. Sh C, Mori D, Kobayashi H, Mori Y, Nakamoto H, Okada K, *et al.* Excessive mechanical loading promotes osteoarthritis through the gremlin-1-NF-κB pathway. *Nat Commun*. 2019;**10**:1442. https://doi.org/10.1038/s41467-019-09491-5.
23. Brooks GA. The science and translation of lactate shuttle theory. *Cell Metab*. 2018;**27**:757–85. https://doi.org/10.1016/j.cmet.2018.03.008.
24. Brooks GA. Lactate shuttles in nature. *Biochem Soc Trans*. 2002;**30**:258–64. https://doi.org/10.1042/bst0300258.
25. Arra M, Swarnkar G, Ke K, Otero JE, Ying J, Duan X, *et al.* LDHA-mediated ROS generation in chondrocytes is a potential therapeutic target for osteoarthritis. *Nat Commun*. 2020;**11**:3427. https://doi.org/10.1038/s41467-020-17242-0.
26. Haller JM, van der Meulen MCH, Olson S, Anderson D, Marsh JL, Working Z. Posttraumatic osteoarthritis: from basic science to clinical implications. *OTA Int Open Access J Orthop Trauma*. 2023;**6**:e232. https://doi.org/10.1097/OI9.0000000000000232.
27. Zhang F, Zhang B, Wang Y, Jiang R, Liu J, Wei Y, *et al.* An extra-erythrocyte role of haemoglobin body in chondrocyte hypoxia adaption. *Nature*. 2023;**622**:834–41. https://doi.org/10.1038/s41586-023-06611-6.
28. Vaupel P, Schmidberger H, Mayer A. The Warburg effect: essential part of metabolic reprogramming and central contributor to cancer progression. *Int J Radiat Biol*. 2019;**95**:912–9. https://doi.org/10.1080/09553002.2019.1589653.
29. Ganapathy-Kanniappan S, Geschwind JFH. Tumor glycolysis as a target for cancer therapy: progress and prospects. *Mol Cancer*. 2013;**12**:152. https://doi.org/10.1186/1476-4598-12-152.
30. Ganapathy-Kanniappan S. Linking tumor glycolysis and immune evasion in cancer: emerging concepts and therapeutic opportunities. *Biochim Biophys Acta Rev Cancer*. 2017;**1868**:212–20. https://doi.org/10.1016/j.bbcan.2017.04.002.
31. Brooks GA. Lactate as a fulcrum of metabolism. *Redox Biol*. 2020;**35**:101454. https://doi.org/10.1016/j.redox.2020.101454.
32. Domínguez R, Maté-Muñoz JL, Serra-Paya N, Garnacho-Castaño MV. Lactate threshold as a measure of aerobic metabolism in resistance exercise. *Int J Sports Med*. 2018;**39**:163–72. https://doi.org/10.1055/s-0043-122740.
33. Patgiri A, Skinner OS, Miyazaki Y, Schleifer G, Marutani E, Shah H, *et al.* An engineered enzyme that targets circulating lactate to alleviate intracellular NADH:NAD+ imbalance. *Nat Biotechnol*. 2020;**38**:309–13. https://doi.org/10.1038/s41587-019-0377-7.
34. Chen P, Liu X, Gu C, Zhong P, Song N, Li M, *et al.* A plant-derived natural photosynthetic system for improving cell anabolism. *Nature*. 2022;**612**:546–54. https://doi.org/10.1038/s41586-022-05499-y.
35. Benítez-Muñoz JA, Cupeiro R, Rubio-Arias JÁ, Amigo T, González-Lamuño D. Exercise influence on monocarboxylate transporter 1 (MCT1) and 4 (MCT4) in the skeletal muscle: a systematic review. *Acta Physiol Oxf Engl*. 2024;**240**:e14083. https://doi.org/10.1111/apha.14083.
36. Schmiedeknecht K, Kaufmann A, Bauer S, Venegas SF. L-lactate as an indicator for cellular metabolic status: an easy and cost-effective colorimetric L-lactate assay. *PLoS One*. 2022;**17**:e0271818. https://doi.org/10.1371/journal.pone.0271818.
37. Moreno-Yruela C, Zhang D, Wei W, Bæk M, Liu W, Gao J, *et al.* Class I histone deacetylases (HDAC1-3) are histone lysine delactylases. *Sci Adv*. 2022;**8**:eabi6696. https://doi.org/10.1126/sciadv.abi6696.
38. Seto E, Yoshida M. Erasers of histone acetylation: the histone deacetylase enzymes. *Cold Spring Harb Perspect Biol*. 2014;**6**:a018713. https://doi.org/10.1101/cshperspect.a018713.
39. Okae H, Toh H, Sato T, Hiura H, Takahashi S, Shirane K, *et al.* Derivation of human trophoblast stem cells. *Cell Stem Cell*. 2018;**22**:50–63.e6. https://doi.org/10.1016/j.stem.2017.11.004.
40. Emans PJ, Spaapen F, Surtel DAM, Reilly KM, Cremers A, van Rhijn LW, *et al.* A novel *in vivo* model to study endochondral bone formation; HIF-1alpha activation and BMP expression. *Bone*. 2007;**40**:409–18. https://doi.org/10.1016/j.bone.2006.08.005.
41. Zhang J, Hu W, Zou Z, Li Y, Kang F, Li J, *et al.* The role of lipid metabolism in osteoporosis: clinical implication and cellular mechanism. *Genes Dis*. 2023;**11**:101122. https://doi.org/10.1016/j.gendis.2023.101122.
42. Gaffney DO, Jennings EQ, Anderson CC, Marentette JO, Shi T, Schou Oxvig AM, *et al.* Non-enzymatic lysine Lactoylation of glycolytic enzymes. *Cell Chem Biol*. 2020;**27**:206–213.e6. https://doi.org/10.1016/j.chembiol.2019.11.005.
43. Guilak F, Nims RJ, Dicks A, Wu CL, Meulenbelt I. Osteoarthritis as a disease of the cartilage pericellular matrix. *Matrix Biol J Int Soc Matrix Biol*. 2018;**71-72**:40–50. https://doi.org/10.1016/j.matbio.2018.05.008.
44. Gyanwali B, Lim ZX, Soh J, Lim C, Guan SP, Goh J, *et al.* Alpha-ketoglutarate dietary supplementation to improve health in humans. *Trends Endocrinol Metab TEM*. 2022;**33**:136–46. https://doi.org/10.1016/j.tem.2021.11.003.

Downloaded from academic.oup.com/burnstrauma/article/doi/10.1093/burnst/tkaf073/8315826 by guest on 12 October 2026

© The Author(s) 2025. Published by Oxford University Press. This is an Open Access article distributed under the terms of the Creative Commons Attribution-NonCommercial License (https://creativecommons.org/licenses/by-nc/4.0/), which permits non-commercial re-use, distribution, and reproduction in any medium, provided the original work is properly cited. For commercial re-use, please contact reprints@oup.com for reprints and translation rights for reprints. All other permissions can be obtained through our RightsLink service via the Permissions link on the article page on our site—for further information please contact journals.permissions@oup.com.
Burns & Trauma, 2026, 14, tkaf073
https://doi.org/10.1093/burnst/tkaf073
Research Article